J. Fluid Mech. (1989), *vol.* 200, *pp.* 389–407
Printed in Great Britain

Second-order recombination in a parallel shear flow

By RONALD SMITH

Department of Applied Mathematics and Theoretical Physics, University of Cambridge, Silver Street, Cambridge CB3 9EW, UK

(Received 5 February 1988 and in revised form 29 April 1988)

For a reactive solute, with weak second-order recombination, an investigation is made of the near-source behaviour (where concentrations are high), and of the far field (where the recombination has an accumulative effect). Despite the loss of material and increased spread due to recombination, the far-field concentration distribution is shown to be nearly Gaussian. This permits a simplified (Gaussian) treatment of the chemical nonlinearity. Explicit solutions are given for the total amount of solute, variance and kurtosis for solutes with no first-order reactions.

1. Introduction

Longitudinal dispersion from a sudden discharge in a parallel shear flow provides an accurate indirect way of measuring small molecular diffusivities (Taylor 1954). This is because the (large) eventual longitudinal spreading rate varies inversely as the (small) molecular diffusivity (Taylor 1953). The values of the diffusivities are of particular importance in chemical reaction processes (such as flames).

For reactive chemical species the longitudinal dispersion process is itself modified by chemical reactions. This is now well-understood when there is a first-order reaction within the flow or at the boundary (Sankarasubramanian & Gill 1973; De Gance & Johns 1978; Lungu & Moffatt 1982; Smith 1983; Barton 1984). The downstream transport velocity and spreading rate can be changed, but the predominant feature is an exponential decrease in concentration.

To compensate for the loss of material the discharge can be prolonged and intensified. However, the possibility then arises of second-order chemical reactions. Motivated by experimental observations, Barton (1986) showed that in various asymptotic regimes, weak second-order recombination can substantially change the concentration distribution (see his figures 1, 2). Not only is there a loss of material, but also there can be an increased rate of spreading. The purpose of the present paper is to give a unified treatment which spans the regimes investigated by Barton (1986).

The premise upon which the present work is based is that, in an appropriate frame of reference, the concentration distribution is nearly Gaussian. So, the mathematical task is reduced to evaluating the extent to which the chemical nonlinearity modifies the area, centroid and variance of the Gaussian. At small times it is important to account for the duration of the discharge (i.e. finite initial concentrations and reaction rates) and it is appropriate to represent the concentrations as being nearly Gaussian with respect to time. At larger times the ubiquitous skewness (Chatwin 1967) can be avoided by the device advocated by Smith (1987) of using tilted axes (an optimal combination of x and t). A measure of the accuracy of the Gaussian approximation is obtained from a calculation of the kurtosis (spikiness).

2. Full equations

To maximize the connection with the cited analyses of first-order reactions we include the possibilities of conversion within the flow and at the boundary. The full equations which we seek to solve are

$$\partial_t c + u\,\partial_x c - \nabla\cdot(\kappa\nabla c) = -\alpha c - \gamma c^2 + q, \tag{2.1a}$$

with

$$\kappa \boldsymbol{n}\cdot\nabla c + \beta c = 0 \quad \text{on} \quad \partial A. \tag{2.1b}$$

Here $c(x,y,z,t)$ is the concentration, $u(y,z)$ is the flow velocity in the longitudinal x-direction, ∇ is the transverse gradient operator $(0,\partial_y,\partial_z)$, $\kappa(y,z)$ is the transverse diffusivity, $\alpha(y,z)$ is the loss rate for a first-order reaction within the flow, $\gamma(y,z)$ is the rate coefficient for the second-order recombination, $q(x,y,z,t)$ is the source strength, $\boldsymbol{n}$ is the outwards normal to the boundary ∂A, and $\beta(y,z)$ is the rate coefficient for the first-order boundary reaction. We have ignored longitudinal diffusion $\kappa\partial_x^2 c$, on the assumption that it is dominated by shear dispersion (Taylor 1953).

The first-order reactions imply that at large times or distances there will be exponential decay (with respect to x or t, or some combination of x and t). In particular if we pose the (x,t)-structure

$$\exp(-\lambda[t+(x-Ut)\,\delta]), \tag{2.2}$$

then the associated (y,z)-dependence satisfies the equations

$$\nabla\cdot(\kappa\nabla\phi) + \lambda[1+(u-U)\,\delta]\,\phi - \alpha\phi = 0, \tag{2.3a}$$

with

$$\kappa\boldsymbol{n}\cdot\nabla\phi + \beta\phi = 0 \quad \text{on} \quad \partial A \tag{2.3b}$$

and

$$\overline{\phi^2} = 1, \ \phi \geqslant 0. \tag{2.3c,d}$$

The particular choices $\delta = 0$ or $\delta = U^{-1}$ make the exponential (2.2) depend on t or x respectively. The natural selection for the advection velocity U is the weighted average

$$U = \overline{u\phi^2}. \tag{2.4}$$

We can factor out the exponential decay, and the reference concentration profile $\phi(y,z)$, by means of the change of variables

$$c = C\phi(y,z)\exp(-\lambda\tau), \tag{2.5a}$$

where

$$\tau = t + (x-Ut)\,\delta, \quad x' = x - Ut. \tag{2.5b,c}$$

The new dependent variable $C(x',y,z,\tau)$ satisfies the equations

$$\phi^2[1+(u-U)\,\delta]\,\partial_\tau C + \phi^2(u-U)\,\partial_{x'} C - \nabla\cdot(\phi^2\kappa\nabla C) = -\gamma\phi^3 C^2\exp(-\lambda\tau) + \phi q\exp(\lambda\tau), \tag{2.6a}$$

with

$$\phi^2\kappa\boldsymbol{n}\cdot\nabla C = 0 \quad \text{on} \quad \partial A. \tag{2.6b}$$

In the special case $\delta = U^{-1}$ the τ-coordinate corresponds to downstream distance x/U. Nothing about the actual concentration distribution can depend on the value of δ. However, the selection of δ does influence the accuracy of the subsequent Gaussian approximation.

The advantage of (2.6a, b) over the original equations (2.1a, b) is that at large times after discharge C becomes uniform across the flow and varies slowly with respect to

both x' and τ. Barton (1986) considers the important limiting case in which there is no first-order reaction and the second-order recombination is weak:

$$\lambda = 0, \quad \phi = 1 \quad \text{with } \gamma \text{ small.} \tag{2.7}$$

3. Hermite series representation

Although we shall eventually be making a Gaussian approximation, we shall embed our calculations in a rigorous framework. To describe the initial behaviour, we regard the discharge as taking place at $\tau = 0$, with centroid at $x' = 0$ and variance ρ^2. The (x', y, z)-dependence of the discharge is represented by a Hermite series:

$$q = \frac{\exp(-\frac{1}{2}\xi^2)}{\rho(2\pi)^{\frac{1}{2}}}\left\{q_0(y,z) + \sum_{m=3}^{\infty} \frac{q_m(y,z)}{\rho^m} \mathrm{He}_m(\xi)\right\}, \tag{3.1a}$$

with

$$\xi = \frac{x'}{\rho}. \tag{3.1b}$$

The Hermite polynomials $\mathrm{He}_m(\xi)$ can be defined recursively:

$$\mathrm{He}_0 = 1, \quad \mathrm{He}_1 = \xi, \quad \mathrm{He}_m = \xi \mathrm{He}_{m-1} - (m-1)\,\mathrm{He}_{m-2}. \tag{3.2}$$

The nature of the discharge may make it appropriate to use a particular value of δ in describing the source and the initial stages. In the special case $\delta = U^{-1}$, (3.1*a*) is a Hermite series with respect to time for a discharge with temporal variance ρ^2/U^2, and positioned at $x = 0$.

In the spirit of the work of Chatwin (1970, 1980) and of Smith (1982), we represent the concentration distribution C for $\tau > 0$:

$$C = \frac{\exp(-\frac{1}{2}\xi^2)}{[2\pi(\sigma^2+\rho^2)]^{\frac{1}{2}}}\left\{a_0(y,z,\tau) + \sum_{m=3}^{\infty} \frac{a_m(y,z,\tau)}{(\sigma^2+\rho^2)^{m/2}} \mathrm{He}_m(\xi)\right\}, \tag{3.3a}$$

with

$$\xi = \frac{x' - X(y,z,\tau)}{(\sigma^2+\rho^2)^{\frac{1}{2}}}. \tag{3.3b}$$

Here $\sigma^2(y,z,\tau)$ is the additional variance, and X the centroid location for $\tau > 0$. The major departures from the work of Barton (1986, §§2, 3) are that there is no restriction to large τ or to $\delta = 0$. In the Gaussian approximation we retain just the a_0 term. The higher-order terms a_3 and a_4 are associated respectively with the skewness and the kurtosis (spikiness). The selection of δ can be used to minimize the skewness at moderate and large times (Smith 1987).

Erdelyi *et al.* (1954, equation 16.5.14) give a formula which permits us to represent the quadratic term C^2:

$$C^2 = \frac{\exp(-\frac{1}{2}\xi^2)}{(\sigma^2+\rho^2)\,\pi\,2\sqrt{2}} \sum_k \sum_l \frac{a_k a_l}{(\sigma^2+\rho^2)^{\frac{1}{2}(k+l)}} \sum_m \frac{I(k,l,m)}{m!} \mathrm{He}_m(\xi). \tag{3.4}$$

The coupling coefficients $I(k,l,m)$ are zero for $k+l+m$ odd, and have the symmetric form

$$I = \frac{\Gamma(s-k)\,\Gamma(s-l)\,\Gamma(s-m)}{\pi^{\frac{3}{2}}} \quad \text{for } k+l+m \text{ even,} \tag{3.5a}$$

with

$$2s = k+l+m+1. \tag{3.5b}$$

In particular, we note that

$$\frac{I(0,0,2n)}{(2n)!} = \frac{(-1)^n}{n!\,2^{2n}}. \tag{3.6}$$

The coefficient of $\mathrm{He}_m(\xi)$ in (2.6a) yields an equation for $a_m(y,z,\tau)$:

$$\begin{aligned}
&\phi^2[1+(u-U)\,\delta]\,\partial_\tau a_m - \nabla\cdot(\phi^2\kappa\nabla a_m)\\
&\quad= \phi^2(u-U-[1+(u-U)\,\delta]\,\partial_\tau X)\,a_{m-1} + 2\phi^2\kappa\nabla X\cdot\nabla a_{m-1} + a_{m-1}\,\nabla\cdot(\phi^2\kappa\nabla X)\\
&\qquad+\tfrac{1}{2}\{\phi^2(2\kappa(\nabla X)^2 - [1+(u-U)\,\delta]\,\partial_\tau\sigma^2)\,a_{m-2}\\
&\qquad+2\phi^2\kappa\nabla\sigma^2\cdot\nabla a_{m-2} + a_{m-2}\,\nabla\cdot(\phi^2\kappa\nabla\sigma^2)\} + a_{m-3}\,\phi^2\kappa\nabla X\cdot\nabla\sigma^2 + \tfrac{1}{4}a_{m-4}\,\phi^2\kappa(\nabla\sigma^2)^2\\
&\qquad-\gamma\phi^3\exp(-\lambda\tau)\,(\sigma^2+\rho^2)^{\frac{1}{2}(m-1)}\sum_k\sum_l \frac{a_k\,a_l}{(\sigma^2+\rho^2)^{\frac{1}{2}(k+l)}}\frac{I(k,l,m)}{m!\,2\pi^{\frac{1}{2}}},
\end{aligned} \tag{3.7a}$$

with $$\phi^2\kappa\boldsymbol{n}\cdot\nabla a_m = 0, \quad \phi^2\kappa\boldsymbol{n}\cdot\nabla X = 0, \quad \phi^2\kappa\boldsymbol{n}\cdot\nabla\sigma^2 = 0 \quad \text{on} \quad \partial A. \tag{3.7b–d}$$

The starting conditions are

$$a_m = b_m, \quad X = 0, \quad \sigma^2 = 0 \quad \text{at} \quad \tau = 0, \tag{3.8a–c}$$

with $$\phi[1+(u-U)\,\delta]\,b_m = q_m. \tag{3.9}$$

The absence of a_1 and a_2 in the series (3.3a) implies that, for $m = 1, 2$, (3.7a–d) define the centroid location X and the additional variance σ^2.

4. Simplified nonlinearity

The most obvious source of complication in (3.7a) is double summation with respect to k and l. To alleviate this, we make the (quasi-Gaussian) approximation of retaining just the $k = l = 0$ contribution. The resulting equations for a_0, T, σ^2 and a_m are

$$\phi^2[1+(u-U)\,\delta]\,\partial_\tau a_0 - \nabla\cdot(\phi^2\kappa\nabla a_0) = -\frac{\gamma\phi^3\exp(-\lambda\tau)\,a_0^2}{(\sigma^2+\rho^2)^{\frac{1}{2}}\,2\pi^{\frac{1}{2}}}, \tag{4.1a}$$

$$\phi^2[1+(u-U)\,\delta]\,\partial_\tau X - 2\phi^2\kappa\frac{\nabla a_0\cdot\nabla X}{a_0} - \nabla\cdot(\phi^2\kappa\nabla X) = \phi^2(u-U), \tag{4.1b}$$

$$\begin{aligned}
&\phi^2[1+(u-U)\,\delta]\,\partial_\tau\sigma^2 - 2\phi^2\kappa\frac{\nabla a_0\cdot\nabla\sigma^2}{a_0} - \nabla\cdot(\phi^2\kappa\nabla\sigma^2)\\
&\qquad= 2\phi^2\kappa(\nabla X)^2 + \gamma\phi^3\exp(-\lambda\tau)\frac{a_0(\sigma^2+\rho^2)^{\frac{1}{2}}}{4\pi^{\frac{1}{2}}},
\end{aligned} \tag{4.1c}$$

$$\begin{aligned}
&\phi^2[1+(u-U)\,\delta]\,\partial_\tau a_m - \nabla\cdot(\phi^2\kappa\nabla a_m)\\
&\quad= 2a_0\,\phi^2\kappa\nabla X\cdot\nabla\left(\frac{a_{m-1}}{a_0}\right) + a_0\,\phi^2\kappa\nabla\sigma^2\cdot\nabla\left(\frac{a_{m-2}}{a_0}\right) + a_{m-3}\,\phi^2\kappa\nabla X\cdot\nabla\sigma^2 + \tfrac{1}{4}a_{m-4}\,\phi^2\kappa(\nabla\sigma^2)^2\\
&\qquad-\frac{\gamma\phi^3\exp(-\lambda\tau)}{4\pi^{\frac{1}{2}}}\left((\sigma^2+\rho^2)^{\frac{1}{2}}\,a_0\,a_{m-2} + \frac{E(\sigma^2+\rho^2)^{n-\frac{1}{2}}(-1)^n\,a_0^2}{n!\,2^{2n-2}}\right).
\end{aligned} \tag{4.1d}$$

The term prefixed E arises only for $m(=2n)$ even.

Various qualitative features can be inferred directly from (4.1a–d). From (4.1a) we see that the loss of material due to recombination is greatest where a_0 is large and $\sigma^2+\rho^2$ is small. At moderate distances downstream of the discharge σ^2 can vary markedly across the flow, being large at the boundary and small where the flow is

fastest. This suggests that there will tend to be an initial depletion of a_0 in the fastest part of the flow.

In (4.1*b*) the $\nabla a_0 \cdot \nabla X$ term enables us to infer that this initial depletion of a_0 in the fastest part of the flow gives a negative contribution to X. All this means physically is that when there is proportionately less material remaining in the fastest part of the flow, the centroid initially moves downstream more slowly.

For the additional variance σ^2, we note that the recombination term on the right-hand side of (4.1*c*) is positive. As revealed by Barton (1986, figures 1, 2), this apparent spreading is consequence of the flattening of the concentration distribution (i.e. greatest depletion near the centroid where the concentration is largest).

Another aspect of this flattening is that for $m = 4$ ($n = 2$) the recombination term in (4.1*d*) gives a negative contribution to a_4. It is the magnitude of the kurtosis

$$A_2 = \frac{4!\, a_4}{a_0(\sigma^2+\rho^2)^2} \tag{4.2}$$

which will give a measure of the accuracy of the quasi-Gaussian approximation.

Following Barton (1986), the remainder of this paper concerns weak recombination, with $\gamma a_0/\bar{u}$ regarded as being small. This limiting case is sufficiently rich to enable us to quantify the features noted above.

5. Recombination near the source for a short pulse

For a comparatively sudden discharge, with ρ small, the high initial concentrations can lead to significant recombination very close to the discharge point. The principal simplification is that for small τ the centroid displacement $X(\tau, y, z)$ can be approximated by

$$X = \frac{\tau(u-U)}{[1+(u-U)\,\delta]}. \tag{5.1}$$

The corresponding small-τ versions of the equations for the amplitude a_0 and the additional variance σ^2 can be written

$$\frac{\partial}{\partial\tau}\left(\frac{a_0}{b_0}\right) = -\frac{\gamma\phi b_0}{[1+(u-U)\,\delta]\,\rho\,2\pi^{\frac{1}{2}}}\left(\frac{a_0}{b_0}\right)^2 \frac{1}{[(\sigma/\rho)^2+1]^{\frac{1}{2}}}, \tag{5.2a}$$

$$\frac{\partial}{\partial\tau}\left(\frac{\sigma^2}{\rho^2}\right) = \frac{2\kappa(\nabla u)^2\tau^2}{[1+(u-U)\,\delta]^5\rho^2} + \frac{\gamma\phi b_0[(\sigma/\rho)^2+1]^{\frac{1}{2}}}{[1+(u-U)\,\delta]\,\rho\,4\pi^{\frac{1}{2}}}\left(\frac{a_0}{b_0}\right). \tag{5.2b}$$

If the $(\nabla u)^2$ shear term in (5.2*b*) was absent, then the growth of $(\sigma/\rho)^2$ would be too slow to keep the chemical reactions from going to completion (i.e. total loss of contaminant). The timescale upon which the shear term becomes important in equation (5.2*b*) can be estimated:

$$\frac{(\rho\gamma\phi b_0)^{\frac{1}{2}}[1+(u-U)\,\delta]^2}{\kappa^{\frac{1}{2}}|\nabla u|}. \tag{5.3a}$$

Thus, we are led to define a dimensionless time coordinate

$$\theta = \frac{\tau|\nabla u|\,\kappa^{\frac{1}{2}}}{[1+(u-U)\,\delta]^2\,(\rho\gamma\phi b_0)^{\frac{1}{2}}}. \tag{5.3b}$$

The corresponding dimensionless measure of the source duration ρ is

$$S = \frac{\rho\kappa(\nabla u)^2}{[1+(u-U)\,\delta]^2\,(\gamma\phi b_0)^3}. \tag{5.4}$$

We note that the local value of S depends strongly upon the local shear (i.e. when the shear is strong there is comparatively little time available for initial recombination, so the effective source duration is large).

The coupled equations (5.2a, b) now become

$$\frac{\partial}{\partial\theta}\left(\frac{a_0}{b_0}\right) = -\frac{1}{S^{\frac{1}{2}}2\pi^{\frac{1}{2}}}\left(\frac{a_0}{b_0}\right)^2\frac{1}{[(\sigma/\rho)^2+1]^{\frac{1}{2}}}, \tag{5.5a}$$

$$\frac{\partial}{\partial\theta}\left(\frac{\sigma^2}{\rho^2}\right) = \frac{2\theta^2}{S^{\frac{1}{2}}} + \frac{[(\sigma/\rho)^2+1]^{\frac{1}{2}}}{S^{\frac{1}{2}}4\pi^{\frac{1}{2}}}\left(\frac{a_0}{b_0}\right) \tag{5.5b}$$

The initial conditions are

$$\frac{a_0}{b_0} = 1, \quad \frac{\sigma^2}{\rho^2} = 0. \tag{5.6a, b}$$

Alternatively, we can eliminate σ^2/ρ^2 to derive a nonlinear second-order differential equation for the concentration ratio $f = a_0/b_0$:

$$\frac{\mathrm{d}^2 f}{\mathrm{d}\theta^2} - \frac{9}{4f}\left(\frac{\mathrm{d}f}{\mathrm{d}\theta}\right)^2 + \frac{4\pi S^{\frac{1}{2}}\theta^2}{f^4}\left(\frac{\mathrm{d}f}{\mathrm{d}\theta}\right)^3 = 0, \tag{5.7a}$$

with

$$f = 1, \quad \frac{\mathrm{d}f}{\mathrm{d}\theta} = -\frac{-1}{S^{\frac{1}{2}}2\pi^{\frac{1}{2}}} \quad \text{at} \quad \theta = 0. \tag{5.7b, c}$$

The asymptotic value at large θ (see figure 1) provides the relationship

$$q_{\mathrm{eff}} = fq \tag{5.8}$$

between the effective and the actual discharge profiles.

It is noteworthy that f varies remarkably little over large changes in S. So, if we were to perform averaging across the flow, the graph of $\bar{f}$ against $\bar{S}$ would be virtually indistinguishable from figure 1.

As an illustrative example, we consider a uniform discharge in Poiseuille pipe flow

$$u = 2\bar{u}\left(1-\left(\frac{r}{a}\right)^2\right), \tag{5.9}$$

with no first-order decay, and with the second-order rate coefficient uniform across the flow (γ = constant). We take $\delta = 1/\bar{u}$, so the discharge is envisaged as taking place at the fixed location $x = 0$ with a temporal spread $\rho/\bar{u}$. The expression (5.3) for S then becomes

$$S(r) = 6\bar{S}\left(\frac{r}{a}\right)^2\left[1-\left(\frac{r}{a}\right)^2\right], \tag{5.10a}$$

where

$$\bar{S} = \frac{16\rho\kappa\bar{u}^2}{3(\gamma q_0)^3 a^2} = \frac{16}{3}\frac{\rho\kappa}{\bar{u}a^2}\left(\frac{\bar{u}}{\gamma q_0}\right)^3. \tag{5.10b}$$

Figure 2 shows the effective discharge distribution, outwards from the centreline of the pipe, for several values of the averaged source duration parameter $\bar{S}$. As well as

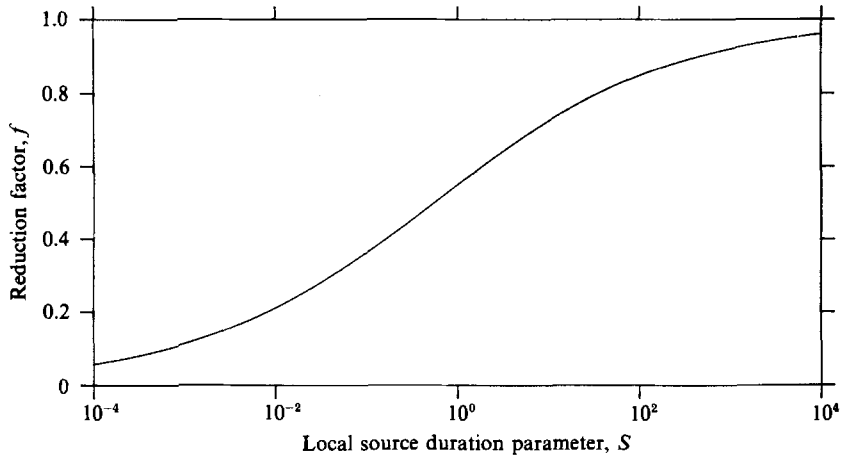

FIGURE 1. The reduction factor f in the effective discharge strength, caused by recombination near the source, as a function of the local source duration parameter S.

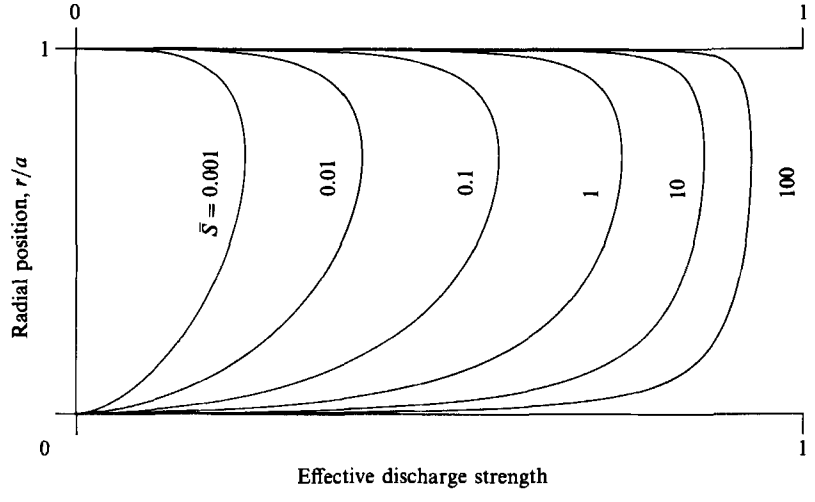

FIGURE 2. The effective discharge profile as modified by recombination near the source, for Poiseuille pipe flow for several values of the cross-sectionally averaged source duration parameter $\bar{S}$.

the anticipated loss of material in the fastest part of the flow, there is also a marked loss near the boundary. This stems from the initially very high concentrations caused by making part of the release in the region of very slow flow.

In terms of the discharge strength q_0, the timescale (5.3a) is of order

$$\frac{(\rho\gamma q_0^{\frac{1}{3}})}{\kappa^{\frac{1}{2}}|\nabla u|}. \tag{5.11}$$

For compatibility with the approximation (5.1) for X, this time must be short compared with the mixing time

$$H^2/\pi^2\kappa, \tag{5.12}$$

were H is the distance between the maximum and minimum velocities (see the Appendix). Thus the quotient

$$\frac{\pi^2(\rho\kappa\gamma q_0)^{\frac{1}{2}}}{H^2|\nabla u|} = \frac{\pi^2\bar{u}}{H|\nabla u|}\left(\frac{\rho\kappa}{\bar{u}H^2}\right)^{\frac{1}{2}}\left(\frac{\gamma q_0}{\bar{u}}\right)^{\frac{1}{2}} = O\left(S^{\frac{1}{2}}\left(\frac{\gamma q_0}{\bar{u}}\right)^2\right) \tag{5.13}$$

must be small (i.e. the pulse length ρ must be short, or the discharge weak).

Barton (1986) uses a small parameter

$$\epsilon = \frac{\gamma q_0}{\bar{u}}. \tag{5.14}$$

So, the above local analysis does indeed pertain to weak recombination provided that the pulse length is not unduly long. In the opposite circumstance in which S is large over most of the flow (e.g. $\bar{S} > 10^4$), the initial recombination is negligible and we can take $f = 1$.

6. Linear solution

Over the mixing time (5.12), we can estimate that the additional variance σ^2 is of order

$$\frac{H^4(\Delta u)^2}{6\pi^3\kappa^2} \tag{6.1}$$

(equation (A 3)). in (4.1a) we can ignore recombination (relative to the ∂_τ term) during the mixing process provided that the quantity

$$\frac{\gamma q_0\sqrt{6}}{\Delta u\, 2\pi} = O\left(\epsilon\frac{\sqrt{6}}{2\pi}\right) \tag{6.2}$$

is small. In this circumstance the mixing process is linear and we can infer that at moderately large τ the amplitude a_0 becomes uniform,

$$a_0 \sim \overline{q_0 f\phi} = a_\infty \tag{6.3}$$

Here a_∞ is a measure of the total amount of contaminant remaining in the flow.

Likewise, from the linear results derived by Smith (1987, (5.8b)), we find that the contaminant distribution eventually moves downstream at the weighted average velocity U, with a centroid displacement function $g(y,z)$ between streamlines:

$$X \sim g(y,z) + \frac{\overline{qf\phi g}}{\overline{qf\phi}} - 2D\delta, \tag{6.4a}$$

where

$$\nabla(\phi^2\kappa\nabla g) = \phi^2(U-u), \tag{6.4b}$$

with

$$\phi^2\kappa\boldsymbol{n}\cdot\nabla g = 0 \quad \text{on} \quad \partial A \tag{6.4c}$$

and

$$\overline{\phi^2 g} = 0. \tag{6.4d}$$

The quantity D is the shear dispersion coefficient (Taylor 1953)

$$D = \overline{(u-U)\phi^2 g} = \overline{\phi^2\kappa(\nabla g)^2}. \tag{6.5}$$

For Poiseuille pipe flow with no first-order decay ($\phi = 1$), the centroid displacement function $g(r)$ is given by

$$g(r) = \frac{\bar{u}a^2}{24\kappa}\left\{2 - 6\left(\frac{r}{a}\right)^2 + 3\left(\frac{r}{a}\right)^4\right\} \quad \text{with} \quad D = \frac{\bar{u}^2a^2}{48\kappa}. \tag{6.6}$$

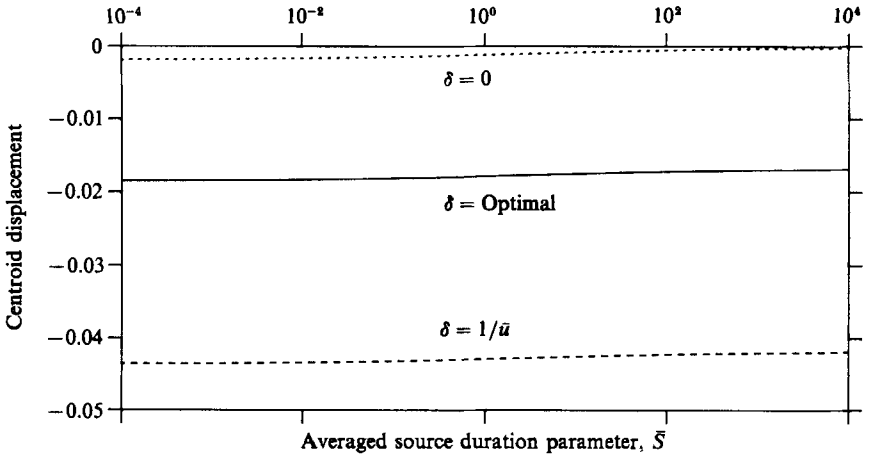

FIGURE 3. The eventual displacement of the centroid position caused by the initial recombination, for Poiseuille pipe flow with a uniform discharge at $x = 0$.

Thus, g is positive in the fastest part of the flow, corresponding to a forwards displacement. Figure 3 shows the dimensionless mean centroid displacement

$$\frac{\kappa}{ua^2}\left\{\frac{\overline{qf\phi g}}{\overline{qf\phi}} - 2D\delta\right\},$$

with q taken to be uniform across the flow. Because the initial depletion takes place both at the centre and at the sides (see figure 2), the centroid displacement is remarkably insensitive to $\bar{S}$. The disparity between the (temporal) $\delta = 0$ and (spatial) $\delta = 1/\bar{u}$ centroids, stems from the fact that the contaminant is continuing to be spread out at the rate $2D$ as it passes a given point (Smith 1987).

From (6.4), or from the Appendix, we can estimate that

$$g \sim \frac{H^2 \Delta u}{\pi^2 \kappa}. \tag{6.7}$$

Thus, in (4.1c) for the additional variance σ^2, the linear and nonlinear forcing terms can be estimated as

$$\frac{H^2(\Delta u)^2}{\pi^4 \kappa} \quad \text{and} \quad \frac{\gamma q_0 H^2 \Delta u}{4\pi^2 \sqrt{6\kappa}}. \tag{6.8a, b}$$

Thus, to neglect recombination during the mixing regime, we require that

$$\frac{\gamma q_0 \pi^2}{\Delta u \, 4\sqrt{6}} = O\left(\epsilon \frac{\pi^2}{4\sqrt{6}}\right) \tag{6.9}$$

be small. Conveniently, this is only marginally more stringent than the estimate (6.2) needed for the linearization of the a_0 equation.

Again, we can simply quote the asymptotic results derived by Smith (1987, (6.14)):

$$\sigma^2 \sim 2\tau D - 4\overline{\phi^2 g^2} + \frac{\overline{qf\phi^2 g^2}}{\overline{qf\phi}} - \left(\frac{\overline{qf\phi g}}{\overline{qf\phi}}\right)^2 + 2\frac{\overline{qf\phi R}}{\overline{qf\phi}} + 2R(y,z) - 2\left(\frac{\overline{qf\phi g}}{\overline{qf\phi}} + g(y,z)\right) D\delta - 6\overline{(u-U)\phi^2 g^2}\,\delta + 8D^2\delta^2, \tag{6.10a}$$

where $$\nabla(\phi^2\kappa\nabla R) = \phi^2 D - \phi^2\kappa(\nabla g)^2, \tag{6.10b}$$

with $$\phi^2\kappa \boldsymbol{n}\cdot\nabla R = 0 \quad \text{on} \quad \partial A, \tag{6.10c}$$

and $$\overline{\phi^2 R} = 0. \tag{6.10d}$$

The eventual linear growth with τ corresponds to Taylor's (1953) constant-dispersion-coefficient model.

To match with the subsequent well-mixed regime, it is convenient to write the asymptote (6.10a) as

$$\sigma^2 = \hat{\sigma}^2 + h, \tag{6.11a}$$

where $$\overline{\gamma\phi^3 h} = 0, \tag{6.11b}$$

and $$\hat{\sigma}^2 + \rho^2 = 2(\tau - \Delta\tau)D. \tag{6.11c}$$

The displacement $\Delta\tau$ between the virtual and actual source is given by

$$2D\Delta\tau = -\rho^2 + 4\overline{\phi^2 g^2} - \frac{\overline{qf\phi^2 g^2}}{\overline{qf\phi}} + \left(\frac{\overline{qf\phi g}}{\overline{qf\phi}}\right)^2 - 2\left(\frac{\overline{qf\phi R}}{\overline{qf\phi}}\right)$$
$$-2\left(\frac{\overline{\gamma\phi^3 R}}{\overline{\gamma\phi^3}}\right) + 2\left(\frac{\overline{qf\phi g}}{\overline{qf\phi}}\right) D\delta + 2\left(\frac{\overline{\gamma\phi^3 g}}{\overline{\gamma\phi^3}}\right) D\delta + 6\overline{(u-U)\,\phi^2 g^2}\,\delta - 8D^2\delta^2. \tag{6.12}$$

If the initial discharge is short we can neglect $-\rho^2$, or if it is long we take $f = 1$.

For Poiseuille pipe flow with no first-order decay ($\phi = 1$) and with the second-order rate coefficient uniform across the flow (γ = constant) we have

$$\left.\begin{aligned} \overline{g^2} &= \frac{\bar{u}^2 a^4}{720\kappa^2}, \quad \overline{(u-\bar{u})\,g^2} = \frac{\bar{u}^3 a^4}{2880\kappa^2}, \\ R &= \frac{\bar{u}^2 a^4}{40320\kappa^2}\left\{74 - 240\left(\frac{r}{a}\right)^2 + 120\left(\frac{r}{a}\right)^4 + 60\left(\frac{r}{a}\right)^6 - 45\left(\frac{r}{a}\right)^8\right\}. \end{aligned}\right\} \tag{6.13}$$

Figure 4 shows the dependence upon the source duration parameter S of the dimensionless displacement $\Delta\tau\kappa/a^2$ for a uniform discharge of short duration (i.e. with $-\rho^2$ neglected). As in figure 3, there is weak dependence upon $\bar{S}$. Again the δ-dependence is a simple consequence of the different (fixed time, fixed position, or mixed) viewpoints of the same evolving concentration distribution.

In this linear regime the departure from a Gaussian distribution is dominated by the a_3 skewness term, which has the asymptotic form

$$\frac{a_3}{a_0} \sim \tau(\overline{(u-U)\,\phi^2 g^2} - 2D^2\delta). \tag{6.14}$$

From the representation (3.3a) the $(\sigma^2+\rho^2)^{\frac{3}{2}}$ term in the denominator implies that the skewness decays as $\tau^{-\frac{1}{2}}$. Thus, far enough downstream the concentration distribution does become Gaussian. However, as emphasized by Chatwin (1970), the approach is at a slow rate.

We are free to choose δ to give alternative representations of the same concentration distribution. The detailed behaviour of the initial discharge merely affect a_∞, and the qf contributions to the centroid position X and to the source

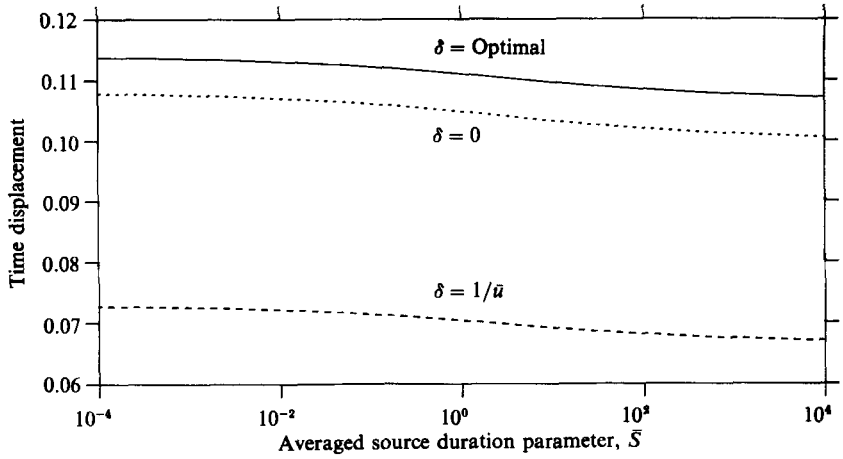

FIGURE 4. The delayed virtual time of discharge as a function of the averaged source duration parameter $\bar{S}$, for Poiseuille pipe flow with a uniform discharge. The positive values indicate the initial inefficiency of the shear-dispersion process.

displacement $\Delta\tau$. Smith (1987) advocates that to give accelerated validity to a Gaussian approximation, we should choose

$$\delta = \frac{\overline{(u-U)\phi^2 g^2}}{2D^2}. \tag{6.15a}$$

For Poiseuille pipe flow with no first-order reactions this optimal selection is

$$\delta = 2/5\bar{u}. \tag{6.15b}$$

7. Nonlinear well-mixed regime

For $\lambda = 0$, Barton (1986) showed that the nonlinear terms eventually have a substantial effect on the concentration distribution. In this well-mixed regime the (y,z)-dependence of a_0 is lost. Thus, the equation (4.1*b*) for the centroid displacement X completely decouples from the other equations. So, the linear asymptote (6.4*a*) remains valid arbitrarily far downstream.

In view of the linear asymptote (6.11*c*) for the total variance $\sigma^2+\rho^2$, we introduce a displaced coordinate

$$\tau^* = \tau - \Delta\tau. \tag{7.1}$$

The parameter δ is implicitly accounted for in the definition (6.12) of $\Delta\tau$. The cross-sectionally averaged versions of (4.1*a*,*c*) are

$$\frac{\mathrm{d}\hat{a}_0}{\mathrm{d}\tau^*} = -\frac{\overline{\gamma\phi^3}\exp(-\lambda\Delta\tau)}{2\pi^{\frac{1}{2}}}\frac{\hat{a}_0^2}{(\hat{\sigma}^2+\rho^2)^{\frac{1}{2}}}\exp(-\lambda\tau^*), \tag{7.2a}$$

$$\frac{\mathrm{d}\hat{\sigma}^2}{\mathrm{d}\tau^*} = 2D + \frac{\overline{\gamma\phi^3}\exp(-\lambda\Delta\tau)}{4\pi^{\frac{1}{2}}}\hat{a}_0(\hat{\sigma}^2+\rho^2)^{\frac{1}{2}}\exp(-\lambda\tau^*). \tag{7.2b}$$

Matching with the linear solution (6.3), (6.11*c*) is equivalent to the imposition of initial conditions at the virtual source:

$$\hat{a}_0 = \overline{q_0 f\phi} = a_\infty, \quad \hat{\sigma}^2+\rho^2 = 0 \quad \text{at} \quad \tau^* = 0. \tag{7.3a,b}$$

A formal scaling with respect to ϵ would suggest that $\lambda\Delta\tau$ be regarded as being of order ϵ^2. For clarity the $\exp(-\lambda\Delta\tau)$ factors will henceforth be replaced by unity. Alternatively, we could absorb the $\exp(-\lambda\Delta\tau)$ factors in a redefinition of γ.

In the absence of first-order decay ($\lambda = 0$), these outer equations can be solved analytically. We introduce a new dimensionless independent variable

$$\xi = \left(\frac{\hat{a}_0}{a_\infty}\right)^{\frac{1}{4}} (\hat{\sigma}^2+\rho^2)^{\frac{1}{2}} \frac{\alpha_\infty \overline{\gamma\phi^3}}{D} \frac{3}{8\pi^{\frac{1}{2}}}, \tag{7.4a}$$

where

$$D\frac{\mathrm{d}\xi}{\mathrm{d}\tau^*} = \left(\frac{\hat{a}_0}{a_\infty}\right)^{\frac{1}{2}} \frac{a_\infty^2(\overline{\gamma\phi^3})^2}{\xi} \frac{9}{64\pi}. \tag{7.4b}$$

The transformed equation for the concentration ratio $(\hat{a}_0/a_\infty)$ is

$$\frac{\mathrm{d}}{\mathrm{d}\xi}\left(\frac{\hat{a}_0}{a_\infty}\right) = -\frac{4}{3}\left(\frac{\hat{a}_0}{a_\infty}\right)^{\frac{7}{4}} \exp(-\lambda\tau^*), \tag{7.5}$$

with

$$\tau^* \frac{a_\infty^2(\overline{\gamma\phi^3})^2}{D} = \frac{64\pi}{9} \int_0^\xi \xi' \left(\frac{\hat{a}_0}{a_\infty}\right)^{-\frac{1}{2}} \mathrm{d}\xi'. \tag{7.5b}$$

For $\lambda = 0$ the solution can be written

$$\frac{\hat{a}_0}{a_\infty} = [1+\xi]^{-\frac{4}{3}}, \tag{7.6a}$$

$$(\hat{\sigma}^2+\rho^2)\frac{a_\infty^2(\overline{\gamma\phi^3})^2}{D^2} = \frac{64\pi}{9}\xi^2[1+\xi]^{\frac{8}{3}}, \tag{7.6b}$$

$$\tau^* \frac{a_\infty^2(\overline{\gamma\phi^3})^2}{D} = \frac{8\pi}{3}([1+\xi]^{\frac{8}{3}} - \tfrac{8}{5}[1+\xi]^{\frac{5}{3}} + \tfrac{3}{5}). \tag{7.6c}$$

The three regimes investigated by Barton (1986, §§3–5) are spanned by ξ small, moderate and large. The nonlinearity of (7.6c) means that the corresponding range of non-dimensional times is extremely large (e.g. with $\xi = 5.7$, (7.6c) yields a dimensionless time of 1000).

The large-ξ asymptotes yield the result

$$\hat{a}_0 \overline{\gamma\phi^3} \sim \left(\frac{8\pi}{3}\right)^{\frac{1}{2}} \left(\frac{D}{\tau^*}\right)^{\frac{1}{2}} = 2.894 \left(\frac{D}{\tau^*}\right)^{\frac{1}{2}}. \tag{7.7}$$

From his nonlinear similarity solution (Barton (1986, §5) obtained the numerical coefficient 2.904. Thus, the present simplified treatment of the nonlinearity is remarkably accurate. It is also noteworthy that the asymptotic solution for the total variance is

$$\hat{\sigma}^2+\rho^2 \sim \tfrac{8}{3}D\tau^*. \tag{7.8}$$

Thus, the apparent shear dispersion coefficient is $\frac{4}{3}D$, and the spread is systematically greater than in the non-reactive case.

For λ non-zero, it is an elementary computational task to integrate (7.5a, b). Figures 5, 6 give plots of the dimensionless amplitude and excess variance

$$\frac{\hat{a}^0}{a_\infty}, \quad (\hat{\sigma}^2+\rho^2-2D\tau^*)\frac{a_\infty^2(\overline{\gamma\phi^3})^2}{D^2}, \tag{7.9a, b}$$

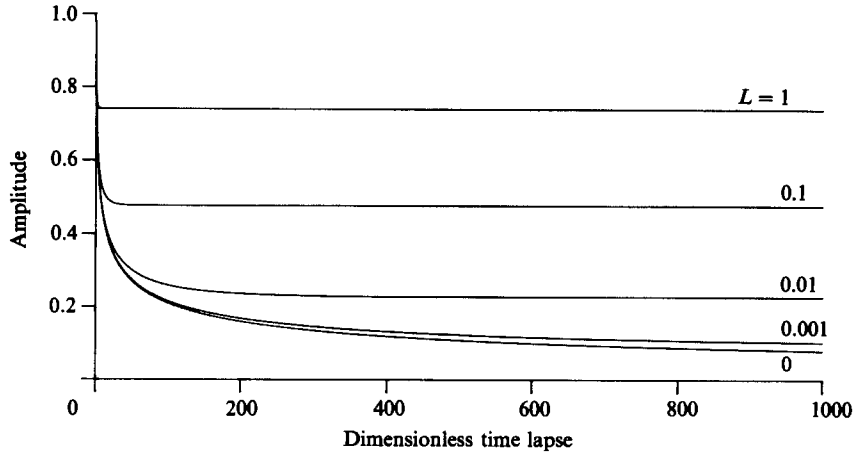

FIGURE 5. Relative loss of material at large times attributable to second-order recombination, for several values of the dimensionless first-order decay rate L. (The first-order exponential decay has been factored out.)

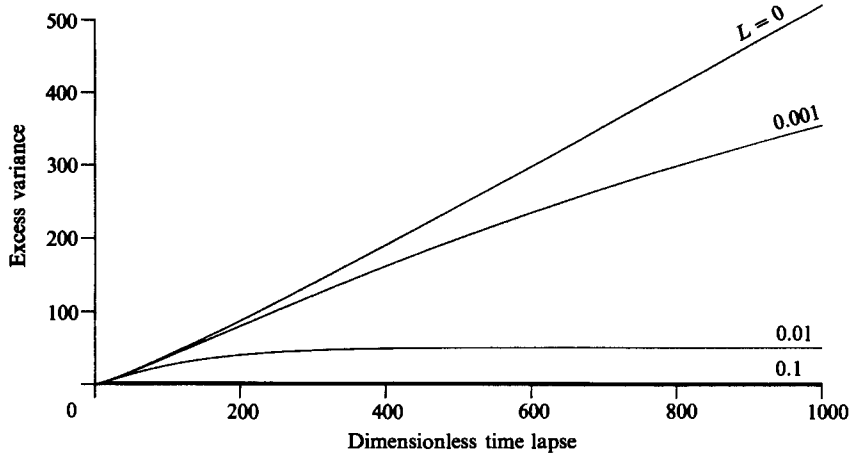

FIGURE 6. Excess variance (beyond the linear diffusive spreading) at large times, for several values of the dimensionless first-order decay rate L.

as functions of the dimensionless time lapse and first-order decay rate

$$\tau^* \frac{a_\infty^2 (\overline{\gamma\phi^3})^2}{D}, \quad L = \frac{\lambda D}{a_\infty^2 (\overline{\gamma\phi^3})^2}. \tag{7.10a,b}$$

We recall that first-order decay has already been accounted for in the change of variable (2.5a). Thus, any reduction in $\hat{a}_0/a_\infty$ can be attributed solely to second-order recombination. Likewise, by virtue of the displacement $\Delta\tau$, the definition (7.9b) of the excess variance relates only to the nonlinearity (with unbounded growth when $\lambda = 0$).

In keeping with the scalings employed by Barton (1986, §§3–5), the non-dimensionalization (7.10a) implies a timescale

$$\frac{D}{a_\infty^2 (\overline{\gamma\phi^3})^2} = \frac{H^2 (\Delta u)^2}{2\pi\kappa a_\infty^2 (\overline{\gamma\phi^3})^2} = O\left(\frac{\pi}{2\epsilon^2} \times \text{mixing time}\right). \tag{7.11}$$

Correspondingly, the non-dimensionalization (7.10*b*) implies a first-order decay exponent

$$\lambda = O(2\epsilon^2/\pi \times \text{mixing time}). \tag{7.12}$$

Thus, as remarked above, $\lambda\Delta\tau$ is formally of order ϵ^2.

For the skewness term $\hat{a}_3$ the far-field equation takes the form

$$\frac{\mathrm{d}}{\mathrm{d}\xi}\left(\frac{\hat{a}_3}{a_\infty}\right) = [\overline{(u-U)\phi^2 g^2} - 2D^2\delta]\frac{64\pi D\xi}{9a_\infty^2(\gamma\phi^3)^2}\left(\frac{\hat{a}_0}{a_\infty}\right)^{\frac{1}{2}}. \tag{7.13}$$

When there is no first-order decay ($\lambda = 0$), the solution is

$$\frac{\hat{a}_3}{a_\infty} = [\overline{(u-U)\phi^2 g^2} - 2D^2\delta]\frac{16\pi D}{3a_\infty^2(\gamma\phi^3)^2}\{(1+\xi)^{\frac{4}{3}} - 4(1+\xi)^{\frac{1}{3}} + 3\} + \text{constant}. \tag{7.14}$$

The constant term matches to the linear solution at $\tau^* = 0$. At extremely large times, we can deduce that

$$\frac{\hat{a}_3}{\hat{a}_0} \approx 2\tau^*[\overline{(u-U)\phi^2 g^2} - 2D^2\delta]. \tag{7.15}$$

There is an extra factor of 2 as compared with the linear result (6.14). We recall that the variance $\sigma^2 + \rho^2$ also grows more rapidly than in the non-reactive case. The net result is that the relative skewness is $3^{\frac{3}{2}}/4 = 1.3$ time is the linear skewness. In either case, the optimal choice (6.15*a*) for δ eliminates the skewness.

8. Kurtosis

In view of Chatwin's (1970) linear calculations and Barton's (1986) nonlinear calculations, we can infer that it is only in the nonlinear outer regime that there can be persistent departures from Gaussianity. The strongest nonlinearity in (4.1*d*) is associated with the E-term, so is associated with $m = (2n)$ even. If we write

$$A_n = \frac{a_{2n}(2n)!}{a_0(\hat{\sigma}^2 + \rho^2)^n}, \tag{8.1}$$

then the dominant terms in (4.1*d*) yield the ordinary differential equations

$$(\hat{\sigma}^2+\rho^2)\frac{\mathrm{d}A_n}{\mathrm{d}\tau^*} + 2n\frac{D}{U^2}A_n = -\frac{\exp(-\lambda\Delta\tau)\,\overline{\phi^3\gamma}}{4\pi^{\frac{1}{2}}}(\hat{\sigma}^2+\rho^2)^{\frac{1}{2}}a_0\exp(-\lambda\tau^*)$$
$$\times\left[(n-2)A_n + 2n(2n-1)A_{n-1} + \frac{(-1)^n(2n)!}{n!\,2^{2n-2}}\right]. \tag{8.2}$$

The $(2n)!$ in the definition (8.1) permits us to identify A_2 as being the Kurtosis (spikiness).

The change of independent variable (7.4*a*, *b*) from τ^* to ξ, and neglecting $\lambda\Delta t^*$, gives the transformed equation

$$\xi\frac{\mathrm{d}A_n}{\mathrm{d}\xi} + 2nA_n = -\tfrac{2}{3}\xi\left(\frac{a_0}{a_\infty}\right)^{\frac{3}{4}}\exp(-\lambda\tau^*)\left[(n-2)A_n + 2n(2n-1)A_{n-1} + \frac{(-1)^n(2n)!}{n!\,2^{2n-2}}\right]. \tag{8.3}$$

For $n = 0, 1$ we have

$$A_0 = 1, \quad A_1 = 0 \tag{8.4a,b}$$

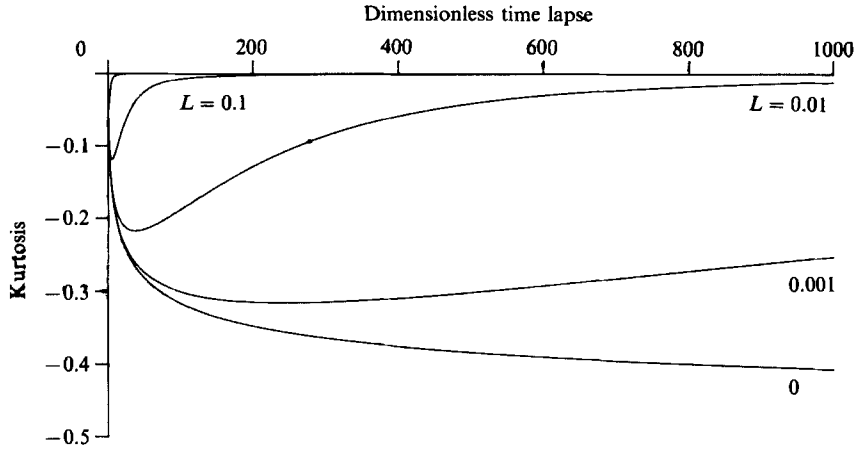

FIGURE 7. Kurtosis (spikiness) at large time, for several values of the dimensionless first-order decay rate L.

and the initial conditions (matching to the linear inner solution) are

$$0 = A_2 = A_3 = \ldots \quad \text{at} \quad \xi = 0. \tag{8.5}$$

In the absence of first-order reactions ($\lambda = 0$), the solution for A_2 is

$$A_2 = -\frac{2}{\xi^4}[\ln(1+\xi) - \xi + \tfrac{1}{2}\xi^2 - \tfrac{1}{3}\xi^3 + \tfrac{1}{4}\xi^4]. \tag{8.6}$$

This solution for the kurtosis is shown in figure 7, together with the numerical solution when there is a first-order decay. The bounding value of $A_2 = -\frac{1}{2}$ corresponds to a $\frac{1}{16}$ reduction in the peak concentration. The relationship (7.6c) between ξ and the non-dimensional time imply that figure 7 only extends out to $\xi = 5.7$, so the asymptote is still quite far from being attained. The accuracy of the quasi-Gaussian approximation (cf. (7.7)) can be attributed to the smallness of the departure from a Gaussian profile. A physical explanation of why the flatness is so slight is that, for weak recombination, there is plenty of time for the concentration distribution to adjust back towards the non-reactive Gaussian form.

9. Effect of recombination on the concentration distribution

If there is no first-order decay ($\lambda = 0$), then the explicit solutions (7.6a, b); (8.2) for the amplitude, variance and kurtosis, make it elementary for us to calculate the concentration distribution. For illustration we consider the fixed large time and short pulse length

$$\frac{t\kappa}{a^2} = 10, \quad \frac{\rho\kappa}{\bar{u}a^2} = 0.01 \tag{9.1a, b}$$

for a uniform discharge in Poiseuille pipe flow. We regard the chemical nature of the material to be fixed

$$\gamma = \text{constant}, \tag{9.2}$$

and we characterize the nonlinearity (i.e. the size of the discharge) by the measure

$$\epsilon = \gamma q_0/\bar{u} \tag{9.3}$$

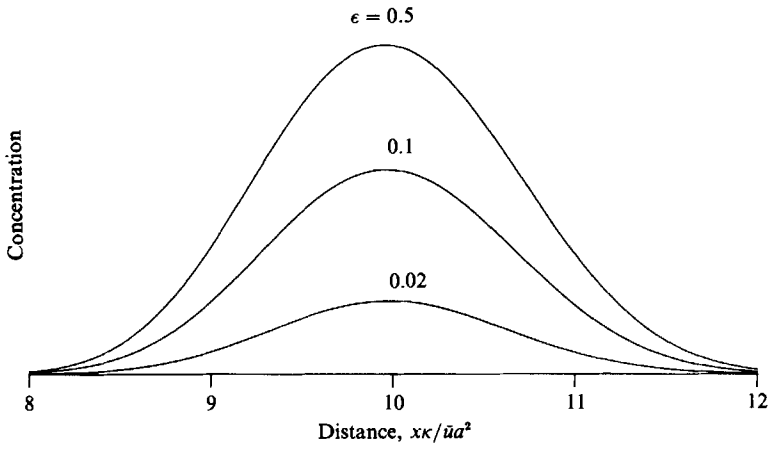

FIGURE 8. Comparison between the longitudinal concentration distribution when the amount of reactive contaminant discharged into the flow is increased by successive factors of 5.

Figure 8 shows the predicted spatial concentration distribution, including skewness and kurtosis, for $\epsilon = 0.02,\ 0.1,\ 0.5$. These values of ϵ span the three regimes investigated by Barton (1986, §§3–5.)

The first step towards determining the profiles is to quantify the loss of contaminant during the initial discharge process. As shown in §5, the crucial quantity is the average source duration parameter:

$$\bar{S} = \frac{16}{3}\frac{\rho\kappa}{\bar{u}a^2}\left(\frac{\bar{u}}{\gamma q_0}\right)^3 = 6667,\quad 53.3,\quad 0.427. \tag{9.4}$$

From figure 1 we can estimate that after the initial recombination the fractional amount of material left in the flow is given by

$$\frac{a_\infty}{q_0} = 0.95,\quad 0.82,\quad 0.48. \tag{9.5}$$

Next, the evolution in the linear regime can be accounted for by means of a centroid displacement and a time displacement. Since we intend to present results at a fixed time, it is convenient to choose $\delta = 0$. From figures 3, 4 we obtain the values

$$\frac{\bar{X}\kappa}{\bar{u}a^2} = -0.0002,\quad -0.0006,\quad -0.0013, \tag{9.6}$$

$$\Delta\tau\frac{\kappa}{a^2} = 0.101,\quad 0.102,\quad 0.104. \tag{9.7}$$

To account for the finite duration ρ of the pulse (see (6.12)), we need to subtract 0.0024 from the latter values (9.7).

For the final nonlinear regime, the dimensionless time lapse (7.10a) can be estimated:

$$48\epsilon^2\left(\frac{a_\infty}{q_0}\right)^2\left(t\frac{\kappa}{a^2} - \Delta\tau\frac{\kappa}{a^2}\right) = 0.17,\quad 3.2,\quad 27. \tag{9.8}$$

From (7.6c), we can determine that the corresponding ξ values are

$$\xi = 0.12,\quad 0.49,\quad 1.27. \tag{9.9}$$

We can use either figure 4, or the formula (7.6*a*) to deduce that the amount of material remaining in the flow has been reduced by the additional factors

$$\frac{\hat{a}_0}{a_\infty} = 0.86, \quad 0.59, \quad 0.34. \tag{9.10}$$

Hence, relative to the original amount q_0, we find that the composite effect of short-term and long-term recombination gives the overall reduction

$$\frac{\hat{a}_0}{q_0} = 0.82, \quad 0.48, \quad 0.16. \tag{9.11}$$

From (7.6*b*) we can calculate that the ξ-values (9.9) correspond to the dimensionless variances

$$\frac{\kappa^2}{\bar{u}^2 a^4}(\hat{\sigma}^2+\rho^2)\left(48\epsilon\frac{a_\infty}{q_0}\right)^2 = 0.347, \quad 7.0, \quad 62.2. \tag{9.12}$$

These results could also be obtained via figure 6 for the dimensionless excess variances. The above results (9.5) for the quotient a_∞/q_0, permit us to get direct estimates for the variance:

$$\frac{\kappa^2}{\bar{u}^2 a^4}(\hat{\sigma}^2+\rho^2) = 0.417, \quad 0.452, \quad 0.469. \tag{9.13}$$

Hence, there is a modest increase in variance with increasing chemical recombination.

If we are to include skewness, then the formula (7.14) yields

$$\frac{\hat{a}_3}{a_\infty}\left(\epsilon\frac{q_\infty}{q_0}\right)^2\left(\frac{\kappa}{a^2\bar{u}}\right)^3 = 1.1\times10^{-6}(1-2.5\bar{u}\delta), \quad 1.6\times10^{-5}(1-2.5\bar{u}\delta), \quad 1.04\times10^{-4}(1-2.5\bar{u}\delta). \tag{9.14}$$

Equivalently, and more usefully,

$$\frac{\hat{a}_3}{\hat{a}_0}\left(\frac{\kappa}{a^2\bar{u}}\right)^3 = 0.0035(1-2.5\delta\bar{u}), \quad 0.0040(1-2.5\delta\bar{u}), \quad 0.0053(1-2.5\delta\bar{u}). \tag{9.15}$$

The small numerical coefficients (as contrasted to those in (9.13)), are indicative of the small skewness at this comparatively large time after discharge.

Finally, for the kurtosis, (8.6) or figure 7 yields

$$A_2 = -0.043, \quad -0.14, \quad -0.25. \tag{9.16}$$

So, the chemical recombination gives a modest flattening of the concentration distribution.

The profiles shown in figure 8 are close to Gaussian, and so justify the simplified (quasi-Gaussian) treatment of the chemical nonlinearity. Increasing the amount of material discharged into the flow by successive factors of 5 does not have a proportional effect upon the concentration. In terms of the longitudinal spreading, the second-order recombination does cause a modest increase in variance. Thus, as a means of measuring κ, there is a loss of accuracy unless allowance is made for the chemical nonlinearity as calculated here or by Barton (1986).

10. Concluding remarks

The main outcome of this paper is a three-stage division of the dispersion process. First there is recombination near the source. The more prolonged the discharge, or the larger the local velocity shear, the more the amount of material that remains unreacted in the flow (i.e. the larger the effective source strength) at the beginning of the second (linear) stage of the dispersion process. During the second stage the weak second-order chemical reactions can be ignored. So, established results on shear dispersion can be used to quantify the adjustments of the centroid and the amount of spread. In particular, a comparison with a constant-dispersion coefficient model (Taylor 1953) permits us to define an effective time of discharge in order to get the same amount of spread. Finally, there is a nonlinear well-mixed regime. The systematic loss of material by recombination where the concentration is high can eventually give a one-third increase in the apparent rate of spreading (and a slightly flattened profile with negative kurtosis). To calculate the concentration distribution at large times, it is necessary to account for all three stages. Recombination near the source determines the effective source strength, linear adjustment determines the effective time origin, and the nonlinear well-mixed regime determines the subsequent evolution.

I wish to thank the Royal Society for financial support.

Appendix. Linear solutions for a simple special case

Powers of π can be important in assessing when the chemical nonlinearity can be ignored. Thus, to guide the estimates we consider the special case

$$u = \bar{u} + \Delta u \cos(\pi y/H), \quad -H < y < H, \tag{A 1}$$

with $\alpha = 0$, $\beta = 0$, $\delta = 0$, $\phi = 1$, $\kappa =$ constant, $q_0 =$ constant.

The solutions for a_0, X and σ^2 are

$$a_0 = q_0, \quad X = \frac{H^2 \Delta u}{\pi^2 \kappa}\{1 - \exp(-\theta)\}\cos\left(\frac{\pi y}{H}\right),$$

$$\sigma^2 = \frac{H^4(\Delta u)^2}{\pi^3 \kappa^3}\{\theta - \tfrac{3}{2} + 2\exp(-\theta) - \tfrac{1}{2}\exp(-2\theta)\}$$

$$- \frac{H^4(\Delta u)^2}{\pi^3 \kappa^2}\{\tfrac{1}{4} - \tfrac{2}{3}\exp(-\theta) + \tfrac{1}{2}\exp(-2\theta) - \tfrac{1}{12}\exp(-4\theta)\}\cos\left(\frac{2\pi y}{H}\right), \tag{A 2}$$

where

$$\theta = \frac{\pi^2 \kappa}{H^2} t.$$

The e-folding rate can be used to define a 'mixing time' corresponding to $\theta = 1$. At this mixing time the cross-sectionally averaged variance is given by

$$\overline{\sigma^2} = \frac{H^4(\Delta u)^2}{\pi^3 \kappa^2} 0.168 \sim \frac{H^4(\Delta u)^2}{6\pi^3 \kappa^2}. \tag{A 3}$$

REFERENCES

BARTON, N. G. 1984 An asymptotic theory for dispersion of reactive contaminants in parallel flow. *J. Austral. Math. Soc.* B **25**, 287–310.

BARTON, N. G. 1986 Solute dispersion and weak second-order recombination at large times in parallel flow. *J. Fluid Mech.* **164**, 289–303.

CHATWIN, P. C. 1970 The approach the normality of the concentration distribution of a solute in solvent flowing along a straight pipe. *J. Fluid Mech.* **43**, 321–352.

CHATWIN, P. C. 1980 Presentation of longitudinal dispersion data. *J. Hydraul. Div. ASCE* **106**, 71–83.

DE GANCE, A. E. & JOHNS, L. E. 1978 The theory of dispersion of chemically active solutes in a rectilinear flow field. *Appl. Sci. Res.* **34**, 189–225.

ERDELYI, A., MAGNUS, W., OBERHETTINGER, F. & TRICOMI, F. G. 1954 *Tables of Integral Transforms*, Vol. II. McGraw Hill.

LUNGU, E. M. & MOFFATT, H. K. 1982 The effect of wall conductance on heat diffusion in duct flow. *J. Engng Maths* **16**, 121–136.

SANKARASUBRAMANIAN, R. & GILL, W. N. 1973 Unsteady convective diffusion with interphase mass transfer. *Proc. R. Soc. Lond.* A **333**, 115–132.

SMITH, R. 1982 Gaussian approximation for contaminant dispersion. *Q. J. Mech. Appl. Maths* **35**, 345–366.

SMITH, R. 1983 Effect of boundary absorption upon longitudinal dispersion in shear flows. *J. Fluid Mech.* **134**, 161–177.

SMITH, R. 1987 Shear dispersion looked at from a new angle. *J. Fluid Mech.* **182**, 447–466.

TAYLOR, G. I. 1953 Dispersion of soluble matter in solvent flowing slowly through a tube. *Proc. R. Soc. Lond.* A **219**, 186–203.

TAYLOR, G. I. 1954 Conditions under which dispersion of a solute in a stream of solvent can be used to measure molecular diffusion. *Proc. R. Soc. Lond.* A **225**, 473–477.